Arabian Journal of Chemistry (2022) **15**, 103723

King Saud University

Arabian Journal of Chemistry

www.ksu.edu.sa
www.sciencedirect.com

ORIGINAL ARTICLE

Bioassay-guided isolation of human carboxylesterase 2 inhibitory and antioxidant constituents from *Laportea bulbifera*: Inhibition interactions and molecular mechanism

Miao-Miao Wang [a,b,c,1], Ya-Nan Li [a,b,c,1], Wei-Kang Ming [a,b,c], Pan-Feng Wu [a,b,c], Ping Yi [a,b,c], Zi-Peng Gong [a,b], Xiao-Jiang Hao [a,b,c,d,*], Chun-Mao Yuan [a,b,c,*]

[a] *State Key Laboratory of Functions and Applications of Medicinal Plants, Guizhou Medical University, Guiyang 550014, People's Republic of China*
[b] *School of Pharmacuetical Sciences, Guizhou Medical University, Guiyang 550025, People's Republic of China*
[c] *Key Laboratory of Chemistry for Natural Products of Guizhou Province, and Chinese Academy of Sciences, Guiyang 550014, People's Republic of China*
[d] *State Key Laboratory of Phytochemistry and Plant Resources in West China, Kunming Institute of Botany, Chinese Academy of Sciences, Kunming 650201, People's Republic of China*

Received 3 November 2021; accepted 19 January 2022
Available online 25 January 2022

KEYWORDS

Laportea bulbifera (Sieb. et. Zucc.) Wedd;
Bioassay-guided isolation;
COX-2 selective inhibitors;
Structure-activity relationships;
Enzyme kinetics;
Molecular simulation

Abstract *Laportea bulbifera* (Sieb. et. Zucc.) Wedd has long been utilized in Traditional Chinese Medicines (TCM) for the treatment of rheumatoid arthritis. However, the study of systematic anti-inflammatory chemical constituents in *L. bulbifera* has never been reported. Thus, bioassay-guided isolation for its roots part led to 46 compounds, including 38 phenolic derivatives. Their structures were determined on the basis of ^{1}H and ^{13}C NMR and MS spectra. All compounds were isolated from *L. bulbifera* for the first time except for 13 compounds. Most of the compounds showed good COX-2 inhibitory activity (IC_{50}: 0.13–3.94 μM) and DPPH radical-scavenging activity (IC_{50}: 1.57–9.55 μM). Four compounds (**4**, **17**, **35**, and **43**) with different skeletons showed preferential COX-2 over COX-1 inhibition with selective indices ranging from 12 to 171. High content active compounds are important for elucidating the basis of the active substance of TCM. Compound **4** (COX-2, IC_{50} 0.24 μM), a high content compound, represented one of the best selective COX-2 inhibitors. Another high content active compound (**35**) with a different skeleton might have

* Corresponding authors.
E-mail addresses: haoxj@mail.kib.ac.cn (X.-J. Hao), yuanchunmao01@126.com (C.-M. Yuan).
[1] These authors contributed equally to this work.

Peer review under responsibility of King Saud University.

Production and hosting by Elsevier

https://doi.org/10.1016/j.arabjc.2022.103723

different mechanism. Further study for the inhibition kinetics against COX-2 indicated compounds **4** and **35** were noncompetitive and competitive COX-2 inhibitors, respectively. Moreover, molecular docking and molecular dynamics simulation data further indicated that compound **4** could bind in the cavity of COX-2 and interacted with key residues VAL-538, PHE-142, and GLY-225 of COX-2 through hydrogen bonds. The results indicated that *L. bulbifera* roots could be applied as antioxidant and anti-inflammatory agents due to their potent selective COX-2 inhibitory and antioxidant activity of phenolic compounds.

1. Introduction

Inflammation is an innate immune response that protects against chemical irritants and foreign antigens, and many diseases can induce inflammatory responses in the human body (Cheung et al., 2002; Jang et al., 2017; Kim et al., 2014). Excessive responses can lead to multiple inflammatory diseases, such as rheumatoid arthritis, systemic lupus erythematosus, and chronic granulomatous disease (Qin et al., 2020). There are multiple mediators of inflammation, and the arachidonic acid cascade in the cyclooxygenase (COX) pathway is one of the important processes. Cyclooxygenase enzymes (COXs) present in two isoforms (constitutive (COX-1) and inducible form (COX-2)) (Puig et al., 2000). COX-2 is a significant target for the discovery of many novel nonsteroidal anti-inflammatory drugs (NSAIDs) (Qin et al., 2020). In contrast, the inhibition for COX-1 could cause adverse gastrointestinal and renal effects (Sağlık, et al., 2021). Therefore, the studies for selective COX-2 inhibitors are important for new drug development. To date, several drugs targeting COX-2 are very popular on the market, such as nimesulide, meloxicam, and celecoxib.

The generation of oxygen free radicals is involved in the occurrence and development of inflammatory-related diseases, such as arthritic disorders and systemic inflammatory response syndrome (Closa and Folch-Puy, 2004; Comhair and Erzurum, 2002). Free radicals are both a cause and a result of inflammation (Chatterjee et al., 2016). Compounds with free radical scavenging activity could to some extent exhibit good anti-inflammatory activity.

Laportea bulbifera (Sieb. et. Zucc.) Wedd, named as Hong Hema, Hong Huoma, Rui Dagun or Wadou, is a perennial herb in the Urticaceae family. It is a folk medicine of Miao and Buyi ethnic minorities in Guizhou Province of China. This plant has long been utilized in traditional Chinese medicines for the treatment of rheumatoid arthritis and some other inflammatory diseases, such as skin itch and sports injury (Editorial Committee of Chinese Flora, 1995; Song et al., 2005). Its extract is usually made in ointments or capsules, such as Runzao Antipruritic Capsules (State Drug Administration, 2002a), Liuwei Shangfuning Ointments (State Drug Administration, 2002a), and Fufang Shangning Ointments (State Drug Administration, 2002b). In particular, Runzao Antipruritic Capsules are very popular on the market in China, and thus were included in the Report on the Scientific and Technological Competitiveness of Large Varieties of Traditional Chinese Medicine (TCM) (Yang et al., 2019). Moreover, its young leaves are edible, and the stem fibers are tough enough to be used in textiles (Editorial Committee of Chinese Flora, 1995). Modern pharmacological studies on this plant indicated that the crude extract exhibited many bioactivities, such as anti-inflammatory (Lu et al., 2012; Chen et al., 2019), immunosuppressive (Xiang et al., 2009), analgesic activities (Su et al., 2009), and anti-rheumatoid arthritis (Luo et al., 2011). Previous phytochemical investigation on *L. bulbifera* indicated the presence of flavonoids (Zhang et al., 2018; Yang et al., 2003), coumarins (Hou et al., 2010), steroids (Zhu et al., 2011), and phenolic acid (Zhu et al., 2011).

Although several scientific studies have indicated that crude extracts of *L. bulbifera* exhibit anti-inflammatory activities *in vitro* and *in vivo* (Wang et al., 2013; Chen et al., 2019), the study of the systematic chemical constituents on the anti-inflammatory effects has never been investigated. To investigate the potential anti-inflammatory compounds in *L. bulbifera*, bioactivity-guided identification of its COX-2 inhibitory and antioxidant compounds was performed. Consequently, bioassay-guided isolation of the ethyl acetate extract led to the isolation and identification of 46 compounds. Most of them exhibited good COX-2 inhibitory and DPPH radical-scavenging activity. Four compounds (**4**, **17**, **35**, and **43**) with different skeletons showed preferential COX-2 over COX-1 inhibition with selective indices (SIs) ranging from 12 to 171. High content active compounds are important for the elucidating the basis of the active substance of TCM. Compound **4** (COX-2, IC_{50} 0.24 μM), a high content compound, represented one of the best selective COX-2 inhibitors. Another high content active compound (**35**) with a different skeleton might have different mechanism. Therefore, these two COX-2 selective inhibitors were selected to study their COX-2 inhibitory mechanism, including their enzyme kinetics, molecular docking, and molecular dynamics.

2. Materials and methods

2.1. General information

Optical rotations were determined on a JASCOP-1020 polarimeter. ^{1}H NMR and ^{13}C NMR spectra were recorded on Bruker Avance NEO 600 spectrometer using TMS as an internal standard. ESI-MS analysis were carried out on Agilent 1100 instrument. Column chromatography was performed on silica gel (300–400 mesh; Qingdao Marine Chemical Co. Ltd., China), Sephadex LH-20 (40–70 μm, Amersham Pharmacia Biotech AB, Uppsala, Sweden), and RP-C18 gel (40–63 μm, Merck, Darmstadt, Germany). Semi-preparative HPLC was performed on an instrument consisting of a Hanbon NP7005c controller, a Hanbon NP7005 pump, and a Hanbon NU3000c UV detector with a YMC-Triart-C18 column (250 × 10.0 mm, 5 μm). Fractions were monitored by TLC (GF 254, Qingdao Marine Chemical Co., Ltd.), and spots were visualized by heating silica gel plates immersed in 5 % H_2SO_4 in ethanol.

2.2. Plant material

The root parts of *Laportea bulbifera* (Sieb. et. Zucc.) Wedd were collected from Libo, Guizhou Province of China, in October of 2019. The identification of the plant was confirmed by Mr. Jun Zhang. A voucher specimen (H20191015) has been preserved in the key laboratory of chemistry for natural products of Guizhou Province and Chinese Academy of Sciences.

2.3. Extraction, isolation and identification of compounds

The air-dried powdered roots of *L. bulbifera* (49 kg) were extracted with 95 % ethanol (EtOH) under reflux for three

times (each time for 3 h). The combined EtOH extracts were concentrated under vacuum to give a crude residue (2.0 kg), which was suspended in water. The water layer was successively partitioned with ethyl acetate (EtOAc) for three times. The EtOAc part (600 g) was separated by a silica gel column chromatography (CC) with CH_2Cl_2/MeOH (99:1, 95:5, 9:1, 8:2, 7:3, 6:4, 1:1, 4:6, 3:7, 2:8, 1:9, v/v) to afford eight fractions (Fr. 1–Fr. 8) after combing a lot of subfractions.

A RP-C18 column was used for fraction 3 (150 g), washed with gradient MeOH/H_2O (50:50, 55:45, 65:35, 75:25, 85:15, 95:5, 100:0, v/v), to give twenty-five subfractions (Fr. 3A-Fr. 3Y). Subsequently, a silica gel column was used for fraction 3B (2.0 g), washed with gradient CH_2Cl_2/acetone (15:1, 10:1, 7:3, v/v) to afford two components (Fr. 3B1 and Fr. 3B2). Fraction 3B1 was subjected to the semi-preparative HPLC eluted with 28 % MeOH/H_2O (2.0 mL/min) to get two compounds (**1**, 100 mg, t_R = 13.3 min; **5**, 80 mg, t_R = 22.0 min). Fraction 3B2 was subjected to the semi-preparative HPLC eluted with 24 % MeOH/H_2O (2.0 mL/min) to get two compounds (**2**, 83 mg, t_R = 11.0 min; **6**, 17 mg, t_R = 19.4 min). Fraction 3 K was separated over Sephadex LH-20 (MeOH) and then chromatographed over a silica gel column eluted with gradient petroleum ether/acetone (20:1, 15:1, 9:1, 7:3, 1:1, v/v) to give five compounds (**25**, 15 mg; **26**, 7 mg; **31**, 6 mg; **27**, 30 mg; **34**, 8 mg). Fraction 3Q was applied to Sephadex LH-20 (MeOH) and chromatographed over silica gel column washed with gradient petroleum ether/EtOAc (40:1, 30:1, 20:1, 9:1, 7:3, 6:1, 1:1, v/v) to give six compounds (**36**, 5 mg; **37**, 11 mg; **38**, 14 mg; **43**, 32 mg; **44**, 23 mg; **46**, 6 mg). Fraction 3Y was applied to a silica gel column eluted with gradient petroleum ether/CH_2Cl_2 (15:1, 10:1, 9:1, 8:2, 7:3, 1:9, v/v) to give five compounds (**39**, 26 mg; **40**, 8 mg; **41**, 13 mg; **42**, 28 mg; **45**, 6 mg).

A RP-C18 column was used for fraction 6 (79 g), washed with gradient MeOH/H_2O (10:90, 20:80, 30:70, 40:60, 50:50, 70:30, 90:10, 100:0, v/v), to obtain ten subfractions (Fr. 6A-Fr. 6 J). Fraction 6A (5 g) was applied to a silica gel column eluted with CH_2Cl_2/MeOH (9:1) to get compound **4** (800 mg). Fraction 6B (4 g) was separated over Sephadex LH-20 (MeOH) to give six fractions (Fr. 6B1-Fr. 6B6). Fraction 6B1 (60 mg) was subjected to the semi-preparative HPLC eluted with 8 % MeOH/H_2O (2.0 mL/min) to get two compounds (**3**, 15 mg, t_R = 26.4 min; **7**, 10 mg, t_R = 52.6 min). Fraction 6B2 (700 mg) was chromatographed over a silica gel column (CH_2Cl_2/acetone, 25:1, 20:1, 15:1, 9:1, v/v) and then subjected to the semi-preparative HPLC eluted with 29 % MeOH/H_2O (2.0 mL/min) to get compound **10** (13 mg, t_R = 37.9 min). Fr. 6B3 (60 mg) was separated over Sephadex LH-20 (MeOH) to give **20** (45 mg). Fr. 6B3 (80 mg) was subjected to the semipreparative HPLC eluted with 50 % MeOH/H_2O (2.0 mL/min) to get **8** (10 mg, t_R = 27.5 min) and **9** (12 mg, t_R = 45.0 min). Fr. 6B5 (10 g) was chromatographed over silica gel eluted with CH_2Cl_2/EtOAc (15:1, 9:1, 7:3, 1:1, v/v) to obtain three fractions (Fr. 6B5A-6B5C). Fr. 6B5C (500 mg) were separated over Sephadex LH-20 (MeOH) to give **32** (25 mg), **33** (13 mg), and **11** (13 mg). Fr. 6C (3.2 g) was separated over Sephadex LH-20 (MeOH) to give seven fractions (Fr. 6C1-Fr. 6C7). Fr. 6C3 (400 mg) was chromatographed over a silica gel column eluted with gradient CH_2Cl_2/MeOH (30:1, 20:1, 10:1, 9:1, 8:2, 1:1, v/v) to obtain four fractions (Fr. 6C3A-Fr. 6C3F). Fr. 6C3A (45 mg) was subjected to the semi-preparative HPLC eluted with 22 % MeOH/H_2O (2.0 mL/min) to get two compounds (**28**, 14 mg, t_R = 18.9 min; **12**, 9 mg, t_R = 25.8 min). Fr. 6C3D was subjected to the semi-preparative HPLC eluted with 18 % MeOH/H_2O (2.0 mL/min) to get three compounds (**13**, 14 mg, t_R = 18.9 min; **29**, 9 mg, t_R = 25.8 min; **21**, 17 mg, t_R = 40.3 min).

Fraction 7 (50 g) was applied to a RP-C18 chromatography column (CC) eluted with a MeOH/H_2O gradient (10:90, 20:80, 30:70, 40:60, v/v) to yield five subfractions (7A–7E). Fraction 7A (5 g) was subjected on a silica gel column, eluted with CH_2Cl_2/MeOH (8:2, v/v) to give five subfractions (Fr. 7A1-Fr. 7A5). Subsequently, Fr. 7A1 (800 mg) was separated on Sephadex LH-20 column (MeOH) to get compound **22** (15 mg) and a major component, which was further purified by semi-preparative HPLC separation to get **14** (21 mg, t_R = 15.6 min), **15** (9.6 mg, t_R = 20.4 min), **23** (14.7 mg, t_R = 23.6 min), **30** (18.9 mg, t_R = 25.7 min), and **16** (13.9 mg, t_R = 35.6 min). Fraction 7B (2.5 g) was applied to a silica gel column and then purified on Sephadex LH-20 (MeOH) to yield two compounds (**35**, 750 mg; **17**, 80 mg). Fraction 7D (3 g) was purified on a silica gel column eluted with gradient CH_2Cl_2/acetone (15:1, 9:1, 7:3, 1:1, 1:9, v/v) to get three compounds (**18**, 12 mg; **19**, 17 mg; **24**, 20 mg).

^1H (400 MHz) and ^{13}C (100 MHz) NMR spectra of all isolates were acquired on a Bruker 400 MHz instrument. Compounds **1**–**46** were identified by comparison of the NMR data with those in the literatures.

2.4. In vitro COX-2 and COX-1 inhibitory assay

The inhibitory activities of the EtOAc and water parts, and all the isolated compounds toward COX-2 were evaluated using the COX-2 Inhibitor Screening Kit (Beyotime, Shanghai, China) (Chen et al., 2019; Jiao et al., 2019; Li et al., 2019). Stock solutions of test samples (the EtOAc and water parts, and all the isolated compounds) were prepared and diluted in DMSO. Celecoxib was used as positive control. According to the manufacturer's protocols, a recombinant human COX-2 enzyme in 96-well plates was incubated with the test samples at varying concentrations for 10 min at 37 ℃. After incubation, the COX-2 probe and substrate were added to each well and incubated for another 15 min at 37 ℃ in the dark. The intensity of the fluorescence was measured using a microplate reader (BioTek) with an excitation wavelength of 560 nm and an emission wavelength of 590 nm.

Inhibition of COX-1 was assessed using a COX fluorescent inhibitor screening assay kit from Cayman Chemical. Stock solutions of test samples were prepared and diluted in DMSO (Mohan et al., 2021; Sağlık, et al., 2021). The inhibition of COX-1 by compounds **4**, **17**, **35** and **43** was analyzed. All reactions were performed in a final volume of 100 µl in 96-well white opaque plate with flat bottom (Cayman) according to the manufacturer's protocol. Briefly, 80 µl of reaction mix were added into each well (including 76 µl COX assay buffer; 1 µl COX probe; 2 µl diluted COX cofactor; 1 µl COX-1). Then, a multi-channel pipette was applied to add 10 µl of diluted arachidonic acid solution into each well to initiate all the reactions at the same time. Fluorescence values with an excitation wavelength of 535 nm and an emission wavelength of 587 nm were tested, using a microplate reader (BioTek) kinetically at 25 ℃ for 10 min.

The inhibitory ratio of COX-1 and COX-2 was calculated by the comparison of the sample treated incubations to control incubations. The IC_{50} values for COX-1 an COX-2 were calculated from the concentration–inhibition response curve.

2.5. Inhibitory kinetic analysis

Kinetic parameter and mechanism analyses of compounds **4** and **35** toward COX-2 were investigated by using Lineweaver-Burk analyses (Liu et al., 2019). The experiments were implemented at different concentrations of arachidonic acid in the absence and presence of compounds **4** (0.06–1.5 μM) and **35** (0.75–3.0 μM), and the data were fitted into Michaelis-Menten plots (Zhao et al., 2021). Moreover, their inhibition type was determined by Lineweaver-Burk analysis (Lin et al., 2019). The kinetic parameters (constant K_i) of compounds **4** and **35** were calculated according to the slope plots and inhibition kinetics model (He et al., 2020).

2.6. Molecular docking

The docking study was performed as described previously (Qin et al., 2020). Molecular docking analysis of COX-2 with compounds **1**–**46** was performed using AutoDock tools (version 1.1.2). The 3-dimensional structures of compounds were prepared using Chem 3D. The coordinates for COX-2 (PDB entry code: 5IKQ) enzyme was obtained from the Protein Data Bank (Qin et al., 2020). Water molecules were removed and polar hydrogens were added for the accurate calculation of partial charges. The grid box size was set at 122, 120, and 114 Å (x, y, and z) with center x = 30.4, y = 48.8, and z = 19.5 for the protein. For further docking, the edited COX-2 and ligand files were transcribed into PDBQT format files. All the parameters were the default. The best docked complex for COX-2 with compounds were selected on the basis of binding free energy value.

2.7. Molecular dynamic simulation

Molecular dynamics (MD) simulation was performed using the GROMACS package for the inhibitor-enzyme interaction mechanism. Compound **4** and 5IKQ were prepared separately according to the coordinates of the docked complex. The protein topology was optimized based on the amber99sb force field (Hornak et al., 2006; Sun et al., 2021). The partial charge of compound **4** was obtained by using the antechamber module of AmberTool. The topology parameters could be generated by the antechamber and ACPYPE programs. A rectangular box with a TIP3P water model was added around the complex with a solvation thickness of at least 1.2 nm. Na ions were added to ensure the neutrality. The production run was performed following proper minimization to fully relax the prepared system. A total 10 ns molecular dynamic trajectory was sampled under isothermal-sobaric condition at 300 K. All the simulations were executed under periodic boundary conditions (PBCs). The enzyme inhibitor interaction at the atomic level was retrieved from the MD trajectory with analytic tools integrated in GROMACS.

2.8. DPPH radical-scavenging assay

A 2,2-diphenyl-1-picrylhydrazyl (DPPH) radical-scavenging assay (Xu et al., 2021) was used to test the antioxidative activity. Five groups, a blank (MeOH), sample (mixed compound and DPPH solution), background (pure compound solution), negative (pure DPPH solution), and positive [mixed vitamin C (V_C) and DPPH solution] controls could be applied for the test. Three tested groups, DPPH (0.15 mM), compounds (1–100 μM), and V_C (1–100 μM), were dissolved in MeOH. Each 160 μl aliquot of MeOH was placed in the negative control and blank groups, while each 160 μl aliquot of the test compounds or V_C was placed in the sample and background groups. MeOH (each 40 μl) was added to the blank and background groups, while 40 μl of DPPH was added to the negative, positive, and sample controls. Then, the absorbance of all tested samples was measured at 517 nm with a microplate reader (Multiskan Spectrum, Thermo Scientific Varioskan LUX) after 30 min of incubation at room temperature. The DPPH radical-scavenging rate was calculated as described in the literature (Xu et al., 2021). The IC_{50} values of the compounds and V_C were calculated by SPSS (Statistical Package for the Social Sciences) software from the radical-scavenging rates at the final concentrations of 10, 5, 2.5, 1.25, 0.625, 0.3125 and 0.155 μg/mL.

2.9. Methods for HPLC

HPLC analysis was performed on a Agilent 1260 instrument using a X-bridge C18 column (5 μm, 4.5 × 250 mm) at 25 ℃ and a flow rate of 0.9 mL/min. The mobile phase components were solvent A (0.1 % phosphoric acid in H_2O, v/v) and solvent B (acetonitrile) using the following gradient: 0–20 min (5–5 % B), 20–45 min (5–10 % B), 45–75 min (10–30 % B), 75–85 min (30–90 % B), 85–95 min (90–90 % B), 95–105 min (90–5 % B), with an injection volume of 10 μl. The ethyl acetate part and each isolate were applied to HPLC with the same condition.

2.10. Statistical Analysis.

All results of bioactivity test were expressed as the mean ± standard deviation (SD) (n = 3). Statistical comparisons were determined by Student *t* test. A P-value of < 0.05 was considered significant. A P-value of < 0.01 was considered highly statistically significant.

3. Results and discussion

3.1. Structure identification of isolated compounds

Using various chromatographic methods, 46 compounds were isolated from the active ethyl acetate (EtOAc) extract of *L. bulbifera* roots. Their structures were elucidated by their spectroscopic data analysis and comparisons with compounds previously reported in the literatures (Fig. 1). These 46 compounds were identified as (+)-catechin (**1**) (Hou et al., 2000), (-)-gallocatechin (**2**) (Foo et al., 2000), (-)-epigallocatechin 3-O-gallate (**3**) (Lee et al., 2000), (-)-epicatechin-3-O-gallate (**4**) (Lin et al., 2011), (+)-

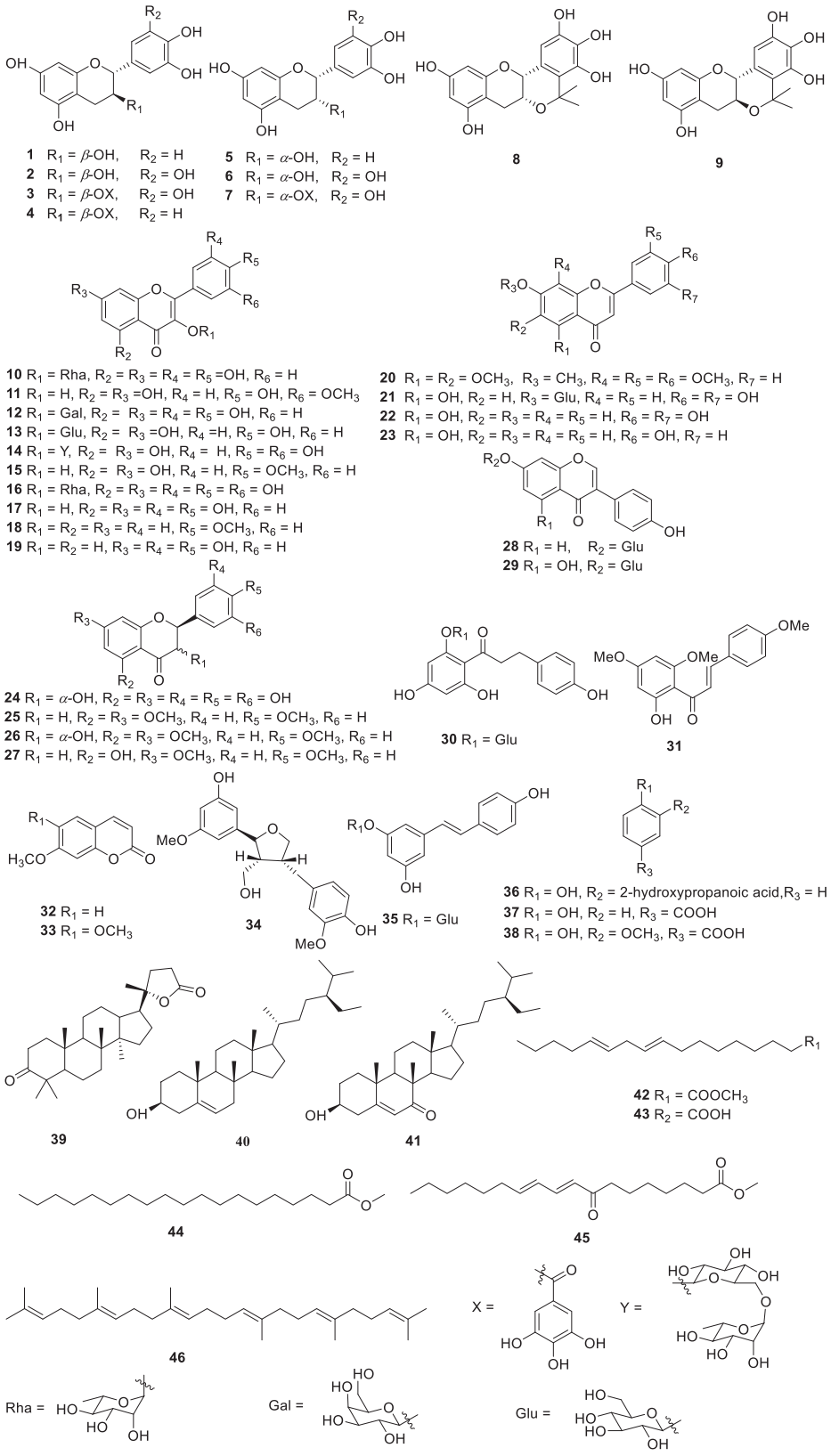

Fig. 1 Chemical structures of isolated compounds.

epicatechin (**5**) (Wei et al., 2013), (-)-epigallocatechin (**6**) (Foo et al., 2000), (-)-gallocatechin 3-O-gallate (**7**) (Choi et al., 2015), (+)-5,5-dimethyl-5,6a,7,12a-tetrahydroisochromeno[4,3-b]chromene-2,3,4,8,10-pentaol (**8**) (Hakamata et al., 2006), (-)-5,5-dimethyl-5,6a,7,12a-tetrahydroisochromeno[4,3-b]chromene-2,3,4,8,10-pentaol (**9**) (Hakamata et al., 2006),

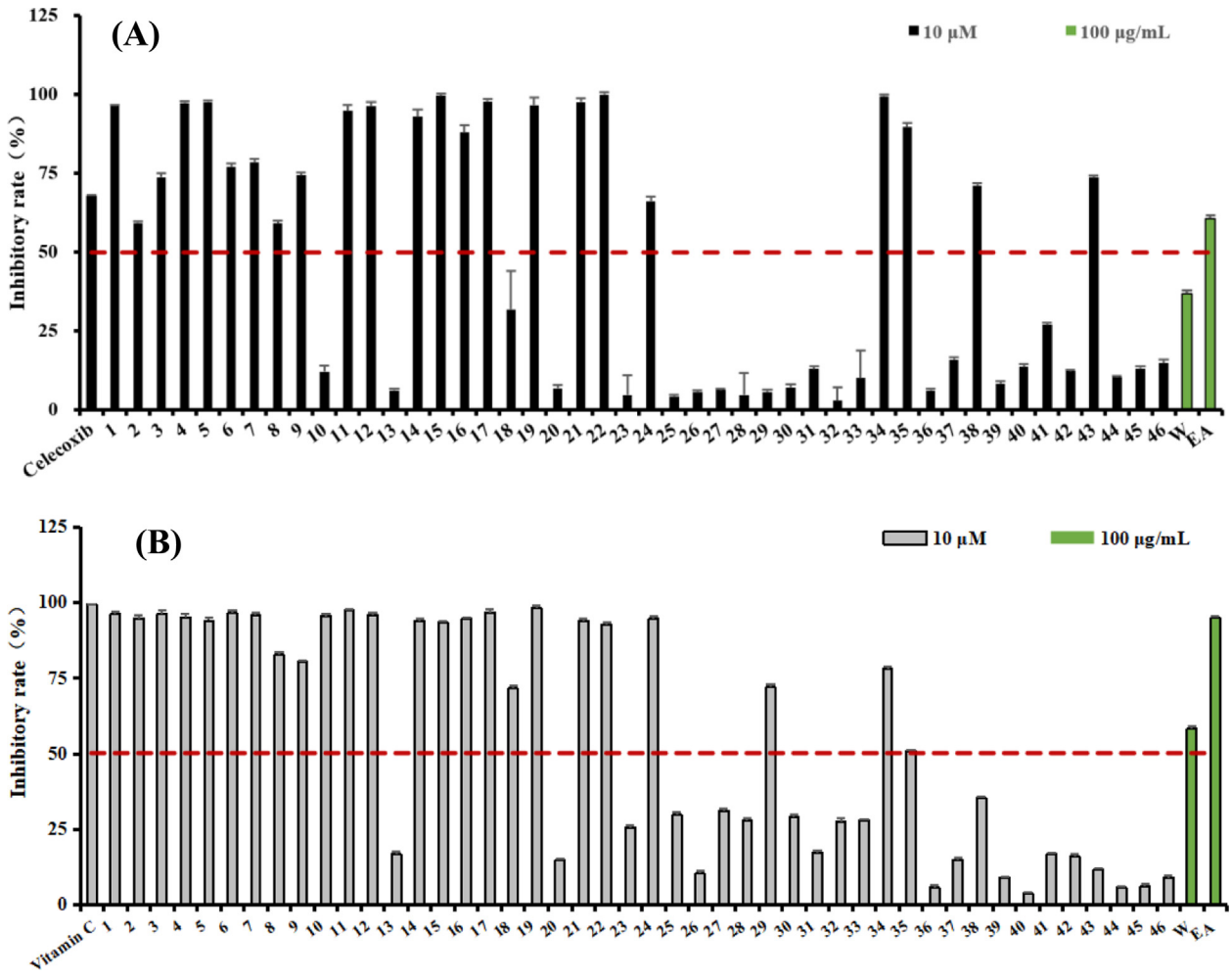

Fig. 2 Effects of extraction and isolates for antioxidant and COX-2 inhibitory activity. (A). COX-2 inhibitory rate for the extraction and isolates; (B). DPPH radical-scavenging inhibitory rate for the extraction and isolates.

quercetin-3-O-rhamnoside (**10**) (Fossen et al., 1999), isorhamnetin (**11**) (Su et al., 2008), hyperoside (**12**) (Isaza et al., 2001), astragalin (**13**) (Xian et al., 2007), rutin (**14**) (Han et al., 2012), kaempferide (**15**) (Zhang et al., 2015), -myricetin-3-O-α-L-rhamnopyranoside (**16**) (Souza et al., 2007), quercetin (**17**) (Guo et al., 2008), 4′-methoxyflavonol (**18**) (Babu et al., 2013), fisetin (**19**) (Mujwah et al., 2010), nobiletin (**20**) (Yue et al., 2013), luteoloside (**21**) (Ma et al., 2007), luteolin (**22**) (Chen et al., 2008), apigenin (**23**) (Tian et al., 2005), (+)-dihydromyricetin (**24**) (Jin et al., 2009), naringenin trimethyl ether (**25**) (Seidel et al., 2000), (+)-4′,5,7-trimethoxydihydroflavonol (**26**) (Zhang et al., 2012), 5-hydroxy-7,4′-dimethoxyflavone (**27**) (Righi et al., 2012), daidzin (**28**) (Kim et al., 2009), genistin (**29**) (Lee et al., 2002a), phloridzin (**30**) (Wang et al., 2008), flavokawain A (**31**) (Seidel et al., 2000), 7-methoxycoumarin (**32**) (Adekenov et al., 2017), scoparone (**33**) (Lee et al., 2002b), (+)-vibruresinol (**34**) (In et al., 2015), piceid (**35**) (Jeong et al., 2010), 2-hydroxy-3-(o-hydroxyphenyl) propanoic acid (**36**) (Wang et al., 1999), p-hydroxybenzoic acid (**37**) (Zou et al., 2006), vanillic acid (**38**) (Geng et al., 2017), (+)-cabralealactone (**39**) (Phongmaykin et al., 2008), β-sitosterol (**40**) (Chundattu et al., 2016), 7-keto-β-sitosterol (**41**) (Yu et al., 2007), methyl linoleate (**42**) (Huh et al., 2010), linoleic acid (**43**) (Marwah et al., 2007), methyl nonadecanoate (**44**) (Capon et al., 1998), methyl (9*E*,11*E*)-8-oxooctadeca-9,11-dienoate (**45**) (Thomas and Pryor, 1980), and squalene (**46**) (Chang et al., 2000). All compounds were isolated from *L. bulbifera* for the first time except for 13 compounds (**1**, **2**, **5**, **6**, **20**, **22**, **33**, **38**, **40**, **41**, **42**, **43**, and **45**). Compounds **1**–**38** are phenolic compounds. Relevant NMR data of all isolates are given in the Supplementary Information. The structures of all compounds are presented in Fig. 1.

3.2. COX-2 inhibitory effects of the extracts and isolates

The preliminary screening of COX-2 inhibitory activity implied that the EtOAc extract showed good COX-2 inhibitory activity with an inhibitory rate of 60.7% at a concentration of 100 μg/ml (Fig. 2A and Table 1). All compounds (**1**–**46**) isolated from the active EtOAc part were tested for COX-2 inhibitory activity at a concentration of 10 μM (Fig. 2B). 23 Compounds (**1**–**9**, **11**, **12**, **14**–**17**, **19**, **21**, **22**, **24**, **34**, **35**, **38**, and **43**) showed good inhibitory rates, higher than

Table 1 COX-2 Inhibitory and antioxidant activities of compounds **1**–**46** and crude extracts.

Compounds	COX-2		DPPH	
	Inhibitory rate (%) [a]	IC_{50} (μM)	Inhibitory rate (%) [a]	IC_{50} (μM)
1	96.34 ± 0.34**[b]	1.40 ± 0.05	96.18 ± 0.86**	2.10 ± 0.06
2	59.29 ± 0.58*	2.08 ± 0.06	94.75 ± 1.02**	2.61 ± 0.11
3	73.78 ± 1.20*	0.46 ± 0.03	96.32 ± 0.99**	1.80 ± 0.16
4	97.33 ± 0.47**	0.24 ± 0.06	95.26 ± 0.85**	1.68 ± 0.05
5	97.58 ± 0.53**	0.56 ± 0.04	94.09 ± 0.81**	2.04 ± 0.12
6	77.06 ± 1.11*	1.97 ± 0.61	96.49 ± 1.09**	1.73 ± 0.09
7	78.51 ± 0.97*	0.70 ± 0.01	95.72 ± 0.74**	1.80 ± 0.27
8	59.16 ± 0.84*	0.97 ± 0.38	82.69 ± 0.99**	3.21 ± 0.13
9	74.36 ± 0.83**	1.73 ± 0.33	80.42 ± 0.62**	2.63 ± 0.24
10	12.09 ± 1.97	–	95.58 ± 0.63**	1.57 ± 0.08
11	94.83 ± 1.92**	3.94 ± 1.14	97.60 ± 0.44**	1.66 ± 0.14
12	96.38 ± 1.34**	0.23 ± 0.01	95.82 ± 0.96**	1.72 ± 0.19
13	6.25 ± 1.45	–	16.77 ± 0.82	–
14	92.87 ± 2.36**	0.22 ± 0.06	94.05 ± 0.66**	1.78 ± 0.30
15	99.57 ± 0.36**	1.29 ± 0.02	93.45 ± 0.37**	1.74 ± 0.22
16	87.89 ± 2.40**	0.35 ± 0.07	94.66 ± 0.51**	1.63 ± 0.16
17	97.79 ± 0.76**	0.13 ± 0.02	96.81 ± 0.92**	2.22 ± 0.14
18	31.87 ± 12.20	–	71.57 ± 0.83*	9.51 ± 0.27
19	96.64 ± 2.51**	0.13 ± 0.01	98.12 ± 0.79**	1.67 ± 0.35
20	12.89 ± 1.13	–	14.74 ± 0.57	–
21	97.58 ± 1.19**	0.36 ± 0.07	93.98 ± 0.63**	1.85 ± 0.38
22	100.00 ± 0.78**	0.17 ± 0.03	92.87 ± 0.69**	3.01 ± 0.11
23	4.79 ± 2.31	–	25.56 ± 0.64	–
24	66.21 ± 1.34*	1.60 ± 0.37	94.73 ± 0.90**	1.69 ± 0.25
25	4.15 ± 0.59	–	29.67 ± 0.85	–
26	5.58 ± 0.56	–	10.31 ± 1.02	–
27	6.28 ± 0.52	–	31.22 ± 0.49	–
28	4.82 ± 1.23	–	27.79 ± 0.87	–
29	5.77 ± 0.79	–	71.99 ± 1.14*	6.23 ± 0.69
30	7.19 ± 0.95	–	29.01 ± 0.95	–
31	12.99 ± 0.78	–	17.17 ± 0.84	–
32	2.96 ± 2.01	–	27.61 ± 0.93	–
33	10.13 ± 2.10	–	27.82 ± 0.65	–
34	99.42 ± 0.49**	0.31 ± 0.02	77.94 ± 0.76*	5.89 ± 0.53
35	89.55 ± 1.49**	1.74 ± 0.03	50.93 ± 0.42*	9.55 ± 0.84
36	6.20 ± 0.51	–	5.90 ± 0.62	–
37	15.99 ± 0.65	–	14.88 ± 0.64	–
38	71.11 ± 0.91**	2.36 ± 0.12	35.34 ± 0.36	–
39	8.32 ± 0.85	–	8.89 ± 0.51	–
40	13.65 ± 0.89	–	3.68 ± 0.31	–
41	26.97 ± 0.85	–	16.75 ± 0.61	–
42	12.22 ± 0.55	–	15.90 ± 0.74	–
43	73.60 ± 0.61*	3.25 ± 0.85	11.63 ± 0.49	–
44	10.38 ± 1.03	–	5.67 ± 0.65	–
45	13.09 ± 0.86	–	6.21 ± 0.76	–
46	14.88 ± 1.03	–	9.04 ± 0.57	–
W [c]	36.92 ± 0.56	–	55.37 ± 0.29*	–
EtOAc [c]	60.67 ± 0.35*	–	92.68 ± 0.25**	–
Celecoxib [d]	67.77 ± 0.12**	0.02 ± 0.001	–	–
Vitamin C [d]	–	–	63.18 ± 0.11**	1.35 ± 0.005

b The results are presented as the mean ± SD of three independent experiments: $^{*}P < 0.05$, $^{**}p < 0.01$ *vs* the blank control.

[a] All compounds were screened at the concentration of 10 μM.

[c] W: Water part; EtOAc, ethyl acetate part; The tested concentration was 100 μg/mL.

[d] Celecoxib is used as the positive control for COX-2 inhibitory assay. Vitamin C is used as the positive control for DPPH inhibitory assay.

50%, at this concentration. Then, these active compounds were tested for their IC_{50}, 13 of which showed strong inhibitory activity with IC_{50} values lower than 1 μM (Table 1). In special, compounds **4**, **12**, **14**, **17**, **19**, and **22** exhibited optimal COX-2 inhibitory potency (IC_{50} values ranging from 0.13 to 0.24 μM).

Table 2 *In Vitro* Inhibition of COX-1 and COX-2 by Compounds **4**, **17**, **35**, and **43**.

Comp.	COX-1 IC_{50} (μM)[a]	COX-2 IC_{50} (μM)	Selectivity Index[b]
4	8.77 ± 0.13	0.24 ± 0.06	37
17	22.22 ± 1.20	0.13 ± 0.02	171
35	21.62 ± 0.65	1.74 ± 0.03	12
43	> 100	3.25 ± 0.85	> 31
Celecoxib	21.52 ± 1.16	0.02 ± 0.001	1076

[a] Results are expressed as the mean of three independent experiments;
[b] Selectivity index = IC_{50}(COX-1)/IC_{50}(COX-2).

3.3. COX-1 inhibitory effects of compounds with different skeletons

The inhibition of COX-1 led to peptic lesions in the gastrointestinal mucosa (Puig et al., 2000). Searching for the selective COX-2 inhibitors could decrease side effects over current novel nonsteroidal anti-inflammatory drugs. Similar skeleton compounds always have similar inhibitory mechanism. Therefore, four most active compounds in their different structural skeletons (**4**, **17**, **35**, and **43**) were selected as representative compounds to test for the COX-1 inhibitory activities. The results indicated that those four compounds showed good COX-2 selectivity index ranging from 12 to 171 (Table 2).

3.4. Inhibition kinetics of two representative compounds against COX-2

High content active compounds are important for the elucidating the basis of the active substance of Traditional Chinese Medicine. Compound **4** (COX-2, IC_{50} 0.24 μM), a high content compound, represented one of the best COX-2 inhibitors among the isolates. Another high content active compound (**35**) with a different skeleton might have different mechanism. Therefore, those two compounds were selected for the the inhibition kinetics against COX-2. This experiment was determined by using Lineweaver-Burk plots to determine their inhibition type (Wang et al., 2018), and the results are shown in Figure 3 and Table 3. As shown in Figure 3, these two compounds (**4** and **35**) revealed COX-2 inhibitory activity in a dose-dependent manner, with IC_{50} values of 0.24 ± 0.06 and 1.74 ± 0.03 μM, respectively. As shown in Figure 3E, a series of lines of compound **4** intersected at a point on the negative X-axis in the Lineweaver-Burk plots, which indicated that the inhibition type of **4** was noncompetitive (He et al., 2020). As shown in Fig. 3F, compound **35** was assigned as a competitive inhibitor since its Lineweaver-Burk plot showed that a series of lines intersected at the Y axis. Thus, compound **4**, a noncompetitive inhibitor, had an inhibition constant K_i value of 0.142 μM by Lineweaver-Burk and slope plots, and compound **35**, a competitive inhibitor, revealed a K_i value of 3.175 μM (Table 3). The K_i values of the two compounds were in good agreement with their COX-2 inhibitory activity (Table 3).

3.5. Molecular docking

Molecular docking was used to predict binding sites between the active compounds and COX-2 (Wang et al., 2010; Zhao

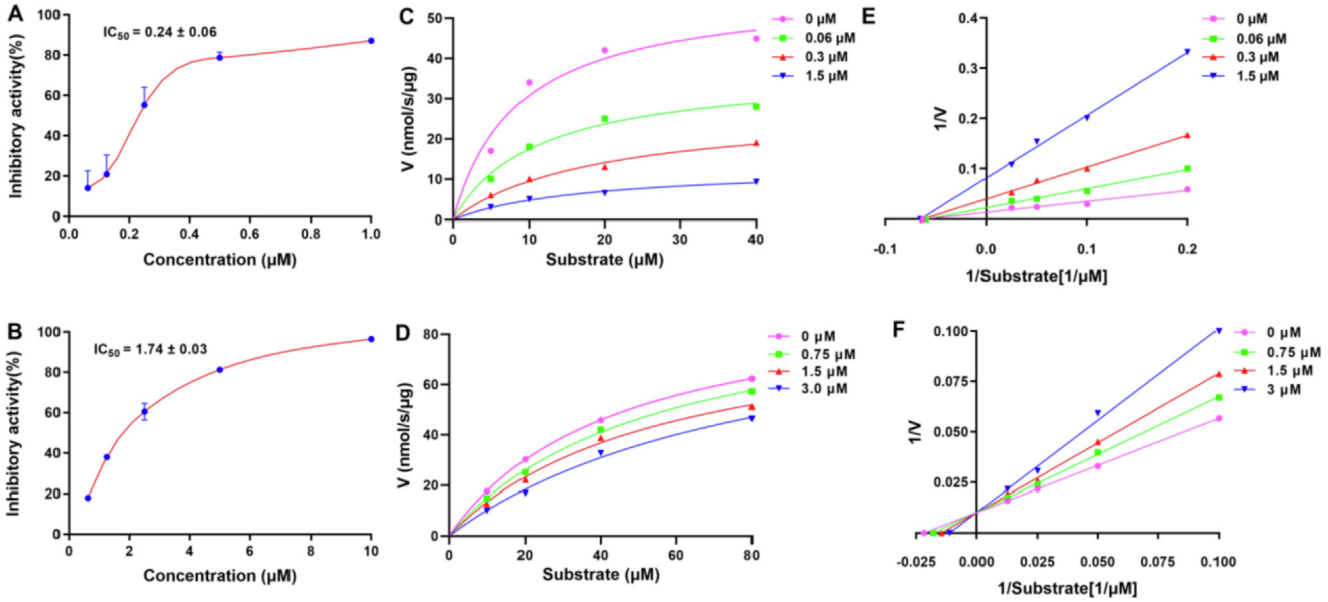

Fig. 3 (A–B) Compounds **4** and **35** displayed concentration-dependent inhibitory activities against COX-2. (C–D) Michealis-Menten plots of compounds **4** and **35** against COX-2. (E-F) Lineweaver-Burk plots of compounds **4** and **35** against COX-2.

Table 3 Kinetic parameters of compounds **4** and **35** against COX-2.

Compounds	Inhibition type	V_{max} (nM/s/μg)	K_m (μM)	K_i (μM)
4	Noncompetitive	57.25	9.73	0.142
35	Competitive	94.94	42.70	3.175

V_{max} is the maximum rate at saturation of the substrate concentration. The unit for V_{max} (nM/s/μg) means per μg protein in per second catalyzed substrate (nmol).

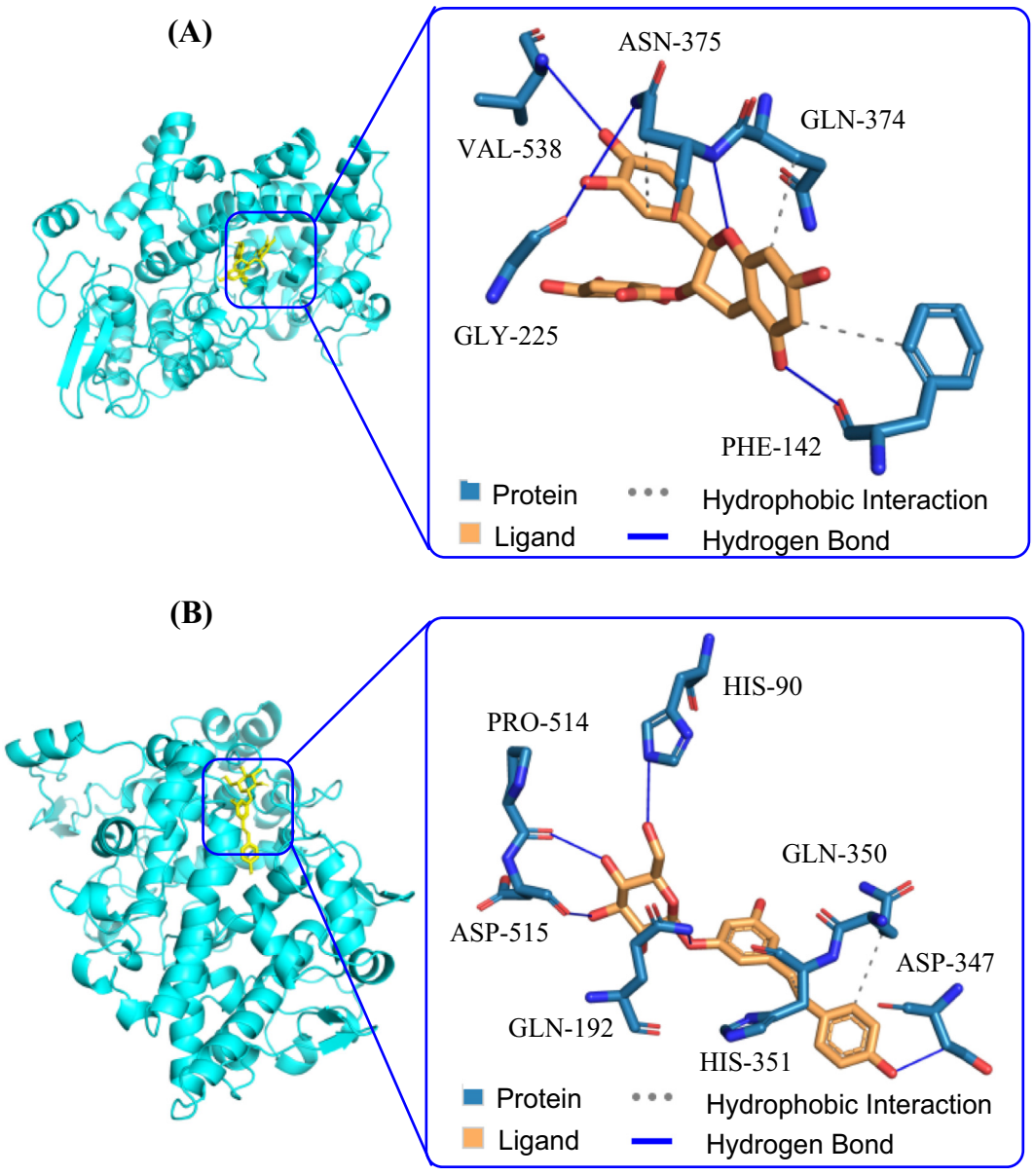

Fig. 4 Binding pose of compounds **4** and **35** with COX-2. (A) The docking study between compound **4** and COX-2; (B) The docking study between compound **35** and COX-2.

et al., 2012). Those two compounds (**4** and **35**) used for the inhibition kinetics were also applied for in silico analysis with a human COX-2 protein model (PDB code: 5IKQ). As shown in Fig. 4A, compound **4** was packed well in the pocket formed by five amino acid residues of the protein, PHE-142, GLY-225, GLN-374, ASN-375, and VAL-538. In Fig. 4B, compound **35** also docked well with the protein, in which five hydrogen bonds were observed between this compound with ASP-347, GLN-192, HIS-90, PRO-514, and ASP-515 of the protein. As shown in Table 4, both compounds had lower bingd energy ranging from −7.5 to −7.8 kcal/mol, confirming their good docking results. Moreover, as shown in Fig. S96 (Supporting Information), arachidonic acid and compound **35** were packed in the same binding site with COX-2, different from that of **4**.

Table 4 Interaction information of compounds **4** and **35** with COX-2.

Comp.	Interaction amino acids	Hydrogen bonds	Binding Energy (kcal/mol)
4	PHE-142, GLY-225, GLN-374, ASN-375, VAL-538	PHE-142, GLY-225, GLN-374, ASN-375, VAL-538	−7.8
35	PRO-514, ASP-515, GLN-192, HIS-351, ASP-347, GLN-350, HIS-90	PRO-514, ASP-515, GLN-192, ASP-347, HIS-90	−7.5

That means those two compounds might have different binding mechanism.

In addition, in order to discuss the relationship between the binding energies and the COX-2 inhibitory activities for all isolates, molecular docking was applied. All the docking results and binding affinity have been summarized in Fig. 5 and Table S1 (Supporting Information). Lower binding energy for docking, higher inhibitory activity for compounds (Rostamian et al., 2020; Rasouli et al., 2020). As shown in Figure 5, 13 compounds (**3**–**5**, **7**–**8**, **12**, **14**, **16**, **17**, **19**, **21**, **22**, and **34)** in green (COX-2: IC_{50} lower 1 μM) had lowest binding energy (Binding affinity < -7 kcal/mol). As for the moderate COX-2 inhibitory active compounds in blue, the binding energies were ranged from −6 kcal/mol to −7 kcal/mol. 23 Compounds in organge in Fig. 5, had higher binding energies than −6 kcal/mol. Obviously, the docking energies are closely related to the COX-2 inhibitory activities.

3.6. Molecular dynamics simulation

Molecular dynamics (MD) has become an important tool to resolve interactions involving enzyme-ligand complexes (Sun et al. 2021). Compound **4** (COX-2, IC_{50} 0.24 μM), a high content compound, represented one of the best COX-2 inhibitors. Thus, this compound was selected for the dynamic interaction with COX-2. As shown in Fig. 6A, a stable complex of compound **4** and COX-2 could form, with the energy of the model system stabilized at approximately -6.7×10^5 kJ/mol. The stability of the simulated complex (compound **4** and COX-2) was screened *via* root mean square deviation (RMSD). The data indicated that the RMSD remained under 2.5 Å during 10 ns of MD simulation, implying a stable simulation run of the tested system (Fig. 6B). The regions with higher flexibility were verified by root mean square fluctuation (RMSF) for the 5IKQ residues (Fig. 6C). Hydrogen bonds between compound **4** and COX-2 were observed in Figure 4, and 9 key amino acid residues, including GLY-225, ASN-375, HIS-226, PHE-142, ASN-537, ARG-376, VAL-538, GLN-374, and GLY-553, were selected to emerge in this MD stimulation (Fig. 6E-F). Moreover, three amino acid residues (VAL-538, PHE-142, and GLY-225) kept close contact with COX-2 through hydrogen bond interactions due to the the calculated distances converging under 3.5 Å during the simulation process, as shown in Fig. 6G. Obviously, this interactions were stable and reliable. These results clarify the role of residues VAL-538, PHE-142, and GLY-225 in the inhibition of compound **4** against COX-2.

3.7. Antioxidant activity

The antioxidant activities of the EtOAc parts and compounds were evaluated using a DPPH radical-scavenging assay, as shown in Fig. 2B and Table 1 (Xu et al., 2021). The active EtOAc part was used for the further phytochemical study. In the DPPH assay, all isolates (**1**–**46**) were screened for the antioxidant activity at a concentration of 10 μM, as shown in Fig. 2B. Among them, 24 compounds (**1**–**12**, **14**–**19**, **21**, **22**, **24**, **29**, **34**, and **35**) revealed great scavenging ability higher than 50%, and had the IC_{50} values lower than 10 μM (Table 1).

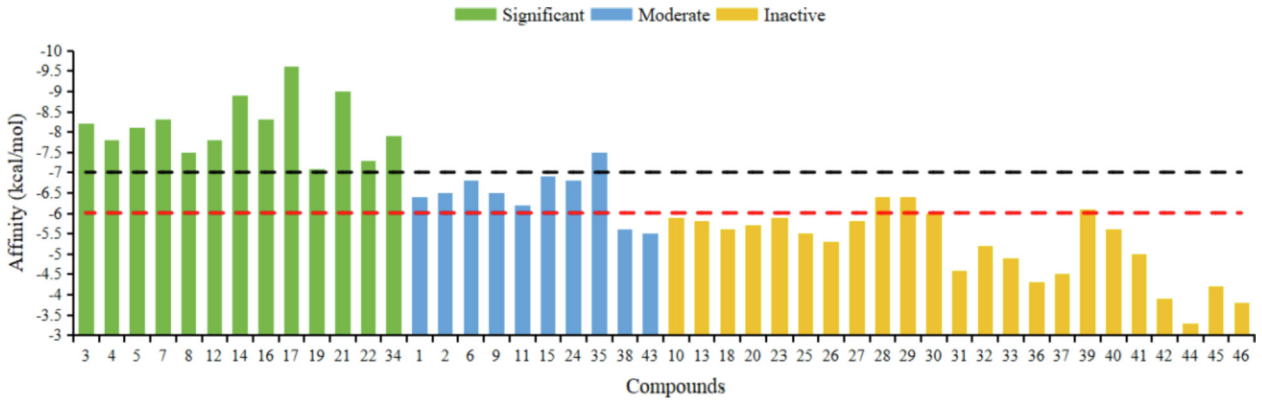

Fig. 5 Binding affinity of compounds **1**–**46**. Significant: compounds with IC_{50} lower 1 μM for COX-2 inhibitory activity. Moderate: compounds with IC_{50} ranging from 1 μM to 10 μM for COX-2 inhibitory activity. Inactive: compounds with IC_{50} higher than 10 μM for COX-2 inhibitory activity.

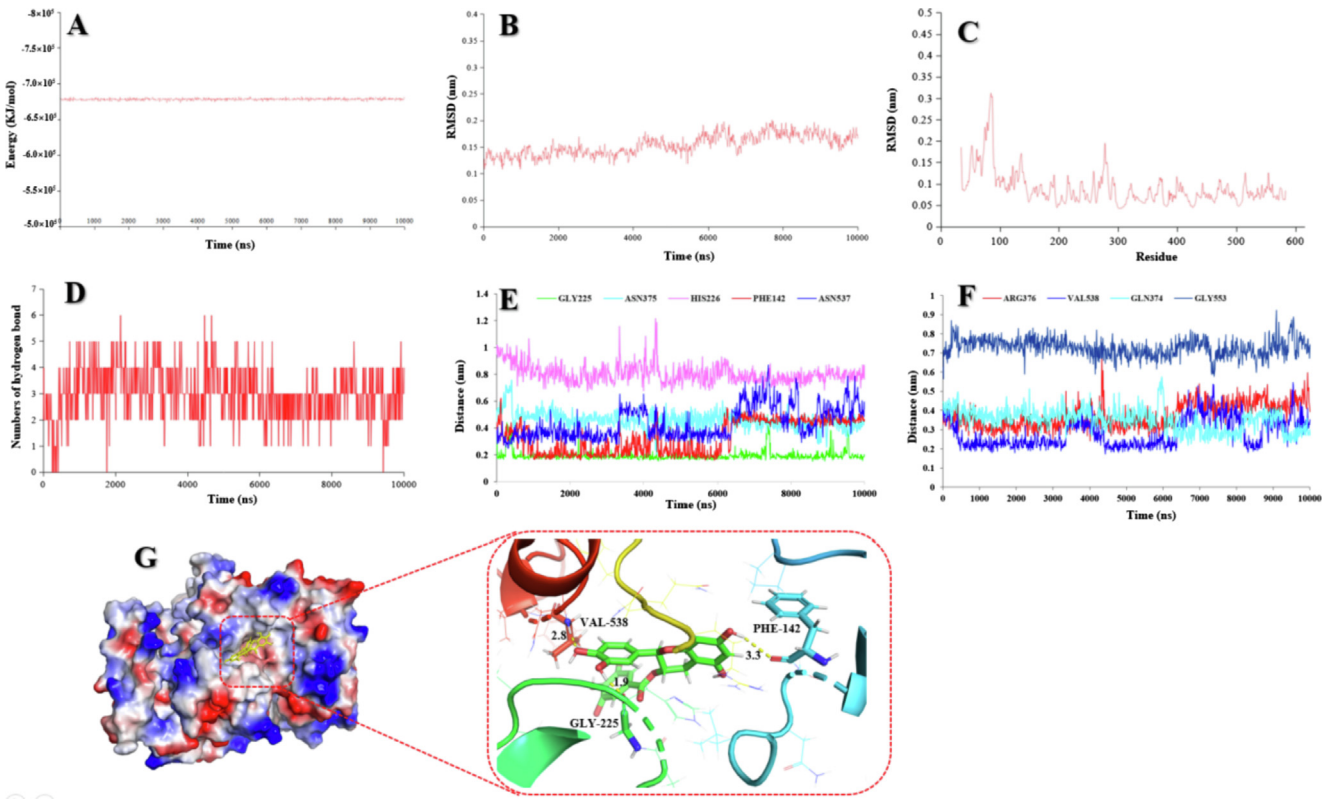

Fig. 6 (A) The potential energy of compound **4** with COX-2 in 10 ns of MD simulation. (B) RMSD of compound **4** with COX-2 in 10 ns of MD simulation. (C) RMSF of compound **4** with COX-2 in 10 ns of MD simulation. (D) The numbers of hydrogen bond in 10 ns of MD simulation. (E) The distances compound **4** with GLY-225, ASN-375, HIS-226, PHE-142, and ASN-537 of COX-2. (F) The distances of compound **4** with ARG-376, VAL-538, GLN-374, and GLY-553 of COX-2. (G) 3D structure of the complex of compound **4** bounded COX-2 and their interaction form in the final frame of 10 ns MD simulation.

3.8. Structure-activity relationships

In the COX-2 inhibitory assay, 23 active compounds could be divided into six structural groups: flavanols (**1**–**9**), flavonoids (**11**, **12**, **14**–**17**, **19**, **21**, **22**, and **24**), lignan (**34**), stilbene (**35**), simple phenol derivatives (**38**), and a fatty acid (**43**). All the flavanols (**1**–**9**) showed good inhibitory activity, and flavanol derivatives with a galloyl group (**3**, **4**, and **7**) exhibited better activity than other compounds without this group (**1**, **2**, and **6**). For the flavonoid derivatives (**10**–**23**), the number of phenolic hydroxyl groups and their position played important roles in the COX-2 inhibitory activity. Although compounds **16** and **17** had the highest numbers of phenolic hydroxyl groups (five phenolic hydroxyl groups), compound **17** exhibited the best COX-2 inhibitory activity (IC_{50}: 0.13 ± 0.02). The difference between these two compounds was only the position of a phenolic hydroxyl group, and therefore, a phenolic group at C-3 (**17**) could improve its activity. The same phenomenon could be observed for the compounds with four phenolic hydroxyl groups (**10**, **11**, **12**, **14**, **19**, and **22**), in which compound **19** with a phenolic group at C-3 was also a best COX-2 inhibitor (IC_{50}: 0.13 ± 0.01). Compounds with different skeletons having one or two phenolic groups (**34**, **35**, and **38**) also revealed good COX-2 inhibitory activity. Four fatty acid derivatives (**42**–**45**) were screened for the COX-2 inhibitory activity, and only compound **43** was active. Obviously, an acid group was important for improving its inhibitory activity among the fatty acid derivatives.

In the DPPH radical-scavenging assay, 24 compounds (**1**–**12**, **14**–**19**, **21**, **22**, **24**, **29**, **34**, and **35**) with phenolic groups revealed significant activity with IC_{50} values lower than 10 μM. Thus, the antioxidant activity is closely related to the number of phenolic hydroxyl groups. These active compounds include six structural types of compounds: flavanols (**1**–**9**), flavonoids (**10**–**12**, **14**–**19**, **21**, and **22**), flavanone (**24**), isoflavone (**29**), lignin (**34**), and stilbene (**35**). All flavanols (**1**–**9**) exhibited good antioxidant activity with IC_{50} values ranging from 1.68 to 3.21 μM, in which compound **4** with seven phenolic groups showed the best activity. Moreover, all the flavonoids expect for compounds **13**, **20**, and **23** with 0 to 3 phenolic groups exhibited good antioxidant activity, which supported the conclusion that the numbers and positions of the phenolic groups were responsible for their activity.

3.9. HPLC analysis

We conducted HPLC analyses of the active EtOAc extract and all the pure isolates (Yuan et al., 2013). The peaks of the EtOAc extract were assigned based on their retention times and UV spectra by comparison of the isolates with the EtOAc extract under the same chromatography conditions (Fig. 7). All the major and minor peaks of the EtOAc part were

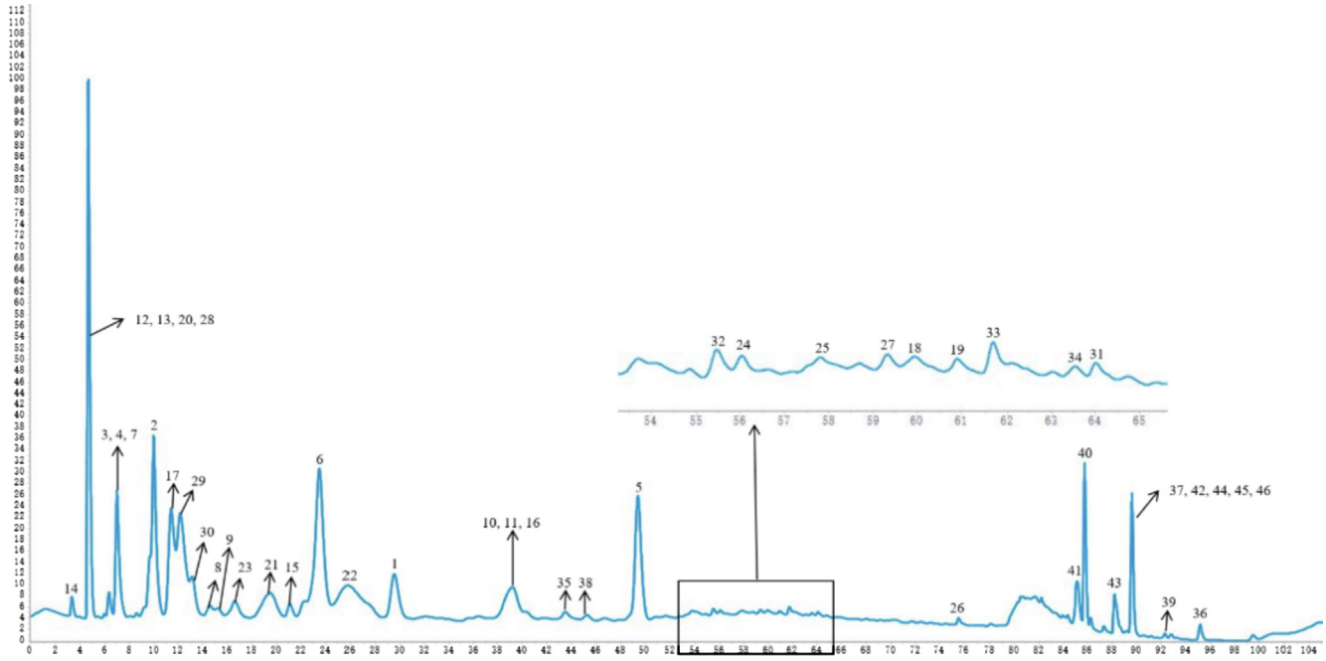

Fig. 7 HPLC spectra of EA extraction (210 nm) and peak identification of all isolates.

assigned, and overlapping compounds were also present in this spectrum. This study, to some extent, elucidated the basis of active substances for this plant.

4. Conclusion

In summary, bioactivity-guided isolation of the roots of *Laportea bulbifera* led to the isolation and identification of 46 compounds using NMR and MS techniques, among which 38 isolates were phenolic derivatives. All isolates were reported for the first time from this plant except for 13 compounds. Most of the compounds showed good COX-2 inhibitory activity (IC_{50}: 0.13–3.94 μM) and DPPH radical-scavenging activity (IC_{50}: 1.57–9.55 μM). Moreover, four compounds (**4**, **17**, **35**, and **43**) with different skeletons showed preferential COX-2 over COX-1 inhibition with selective indices ranging from 12 to 171. Two high content compounds (**4** and **35**) with different skeletons were assigned as noncompetitive and competitive COX-2 inhibitors, respectively. Furthermore, molecular docking and molecular dynamics simulation for compound **4** clarify the role of residues VAL-538, PHE-142, and GLY-225 in the inhibition of compound **4** against COX-2. The chemical fingerprint and structure activity relationship were also investigated. Previous studies implied that crude extracts of *L. bulbifera* exhibit anti-inflammatory activities *in vitro* and *in vivo* (Wang et al., 2013). However, this study found a great deal of phenolic compounds with good COX-2 inhibitory and antioxidant activity. The results indicated that *L. bulbifera* roots could be applied as antioxidant and anti-inflammatory agents.

Declaration of Competing Interest

The authors declare that they have no known competing financial interests or personal relationships that could have appeared to influence the work reported in this paper.

Acknowledgements

The work was financially supported by the National Natural Science Foundation of China (U1812403), the 13th Batch of Outstanding Young Scientific and Technological Talents in Guizhou Province (QKHPTRC [2021]5633), Natural Science and Technology Foundation of Guizhou Province (J[2019]1216), Guiyang Science and Technology Bureau ([2021]43-12), High-level Innovative Talents in Guizhou Province (Thousand Levels of Talent for Chunmao Yuan in 2018), and "Light of the West" Talent Cultivation Program of Chinese Academy of Sciences for Chunmao Yuan (RZ [2020]82).

Appendix A. Supplementary data

Supplementary data to this article can be found online at https://doi.org/10.1016/j.arabjc.2022.103723.

References

Adekenov, S.M., Shaimerdenova, Z.R., Gatilov, Y.V., Atazhanova, G.A., 2017. Two new sesquiterpene lactones from *Artemisia halophila*. Chem. Nat. Compd. 53, 284–289. https://doi.org/10.1007/s10600-017-1971-x.

Babu, M., Pitchumani, K., Ramesh, P., 2013. An expeditious synthesis of flavonols promoted by montmorillonite KSF clay and assisted by microwave irradiation under solvent-free conditions. Helv. Chim. Acta 96, 1269–1272. https://doi.org/10.1002/hlca.201200336.

Capon, R.J., Barrow, R.A., Rochfort, S., Jobling, M., Skene, C., Lacey, E., Gill, J.H., Friedel, T., Wadsworth, D., 1998. Marine nematocides: Tetrahydrofurans from a southern Australian brown alga, *Notheia anomala*. Tetrahedron 54, 2227–2242. https://doi.org/10.1016/S0040-4020(97)10432-X.

Chang, M.H., Wang, G.J., Kuo, Y.H., Lee, C.K., 2000. The low polar constituents from *Bidens pilosa* L. var. Minor (Blume) Sherff. J. Chin. Chem. Soc-Taip. 47, 1131–1136. https://doi.org/10.1002/jccs.200000152.

Chatterjee, S., 2016. Chapter two - oxidative stress, inflammation and disease. In oxidative stress and biomaterials. Oxidative Stress and Biomaterials. Academic Press, pp. 35–58.

Chen, F.Z., Xiang, Q.X., Li, S.H., 2008. Chemical constituents in the leaves of *Alsophila spinulosa*. Acta Bot. Boreali-Occident. Sin. 28, 1246–1249. https://doi.org/10.1016/S1004-9541(08)60026-9.

Chen, Y.R., Zou, S.H., Xu, W.F., Sun, Q.W., Yun, L., 2019. Spectrum–effect relationship of antioxidant and antiinflammatory activities of *Laportea bulbifera* based on multivariate statistical analysis. Biomed. Chromatogr. 34, 1–16. https://doi.org/10.1002/bmc.4734.

Cheung, C.Y., Poon, L.L.M., Lau, A.S., Luk, W., Lau, Y.L., Shortridge, K.F., Gordon, S., Guan, Y., Peiris, J.S.M., 2002. Induction of proinflammatory cytokines in human macrophages by influenza A (H5N1) viruses: a mechanism for the unusual severity of human disease. Lancet 360, 1831–1837. https://doi.org/10.1016/S0140-6736(02)11772-7.

Choi, S.J., Hong, Y.D., Lee, B., Park, J.S., Jeong, H.W., Kim, W.G., Shin, S.S., Yoon, K.D., 2015. Separation of polyphenols and caffeine from the acetone extract of fermented tea leaves (*Camellia sinensis*) using high-performance countercurrent chromatography. Molecules 20, 13216–13225. https://doi.org/10.3390/molecules200713216.

Chundattu, S.J., Agrawal, V.K., Ganesh, N., 2016. Phytochemical investigation of *Calotropis procera*. Arab. J. Chem. 9, S230–S234. https://doi.org/10.1016/j.arabjc.2011.03.011.

Closa, D., Folch-Puy, E., 2004. Oxygen free radicals and the systemic inflammatory response. IUBMB Life 56, 185–191. https://doi.org/10.1080/15216540410001701642.

Comhair, S.A.A., Erzurum, S.C., 2002. Antioxidant responses to oxidant-mediated lung diseases. Am. J. Physiol-Lung. C 283, L246–L255. https://doi.org/10.1152/ajplung.00491.2001.

Editorial Committee of Chinese Flora, 1995. Flora of China. Science Press, Beijing, p. 32. 10.1371/journal.pone.0062794.

Foo, L.Y., Lu, Y., Molan, A.L., Woodfield, D.R., McNabb, W.C., 2000. The phenols and prodelphinidins of white clover flowers. Phytochemistry 54, 539–548. https://doi.org/10.1016/S0031-9422(00)00124-2.

Fossen, T., Larsen, Å., Kiremire, B.T., Andersen, Ø.M., 1999. Flavonoids from blue flowers of *Nymphaèa caerulea*. Phytochemistry 51, 1133–1137. https://doi.org/10.1016/S0031-9422(99)00049-7.

Geng, Y., Zhu, S., Cheng, P., Lu, Z.M., Xu, H.Y., Shi, J.S., Xu, Z.H., 2017. Bioassay-guided fractionation of ethyl acetate extract from *Armillaria mellea* attenuates inflammatory response in lipopolysaccharide (LPS) stimulated BV-2 microglia. Phytomedicine 26, 55–61. https://doi.org/10.1016/j.phymed.2017.01.005.

Guo, N., Chen, X.Q., Zhao, Q.S., 2008. A new polyisoprenylated benzoylphloroglucinol derivative from *Hypericum henryi* subsp. *uraloides* (Guttiferae). Acta Bot. Yunnanica 30, 515–518. https://doi.org/10.3724/SP.J.1143.2008.00515.

Hakamata, W., Nakanishi, I., Masuda, Y., Shimizu, T., Higuchi, H., Nakamura, Y., Saito, S., Urano, S., Oku, T., Ozawa, T., et al, 2006. Planar catechin analogues with alkyl side chains: A potent antioxidant and an α-glucosidase inhibitor. J. Am. Chem. Soc. 128, 6524–6525. https://doi.org/10.1021/ja057763c.

Han, C.H., Leng, A.J., Ying, X.X., 2012. Vitexin and rutin isolation of hawthorn Leaves. Liaoning J. Tradit. Chin. Med. 39, 2028–2030.

He, X., Zhao, W.Y., Shao, B., Zhang, B.J., Liu, T.T., Sun, C.P., Huang, H.L., Wu, J.R., Liang, J.H., Ma, X.C., 2020. Natural soluble epoxide hydrolase inhibitors from *Inula helenium* and their interactions with soluble epoxide hydrolase. Int. J. Biol. Macromol. 158, 1362–1368. https://doi.org/10.1016/j.ijbiomac.2020.04.227.

Hou, A.J., Liu, Y.Z., Yang, H., Lin, Z.W., Sun, H.D., 2000. Hydrolyzable tannins and related polyphenols from *Eucalyptus globulus*. J. Asian Nat. Prod. Res. 2, 205–212. https://doi.org/10.1080/10286020008039912.

Hou, W.R., Su, Z.Q., Pi, H.F., Yao, G.M., Zhang, P., Luo, X., Xie, S. N., Xiang, M., 2010. Immunosuppressive constituents from *Urtica dentata* Hand. J. Asian Nat. Prod. Res. 12, 707–713. https://doi.org/10.1080/10286020.2010.490779.

Hornak, V., Abel, R., Okur, A., Strockbine, B., Roitberg, A., Simmerling, C., 2006. Comparison of multiple Amber force fields and development of improved protein backbone parameters. Proteins: Struct. Funct. Bioinform. 65 (3), 712–725. https://doi.org/10.1002/prot.v65:310.1002/prot.21123.

Huh, S., Kim, Y.S., Jung, E., Lim, J., Jung, K.S., Kim, M.O., Lee, J., Park, D., 2010. Melanogenesis inhibitory effect of fatty acid alkyl esters isolated from *Oxalis triangularis*. Biol. Pharm. Bull. 33, 1242–1245. https://doi.org/10.1248/bpb.33.1242.

In, S.J., Seo, K.H., Song, N.Y., Lee, D.S., Kim, Y.C., Baek, N.I., 2015. Lignans and neolignans from the stems of *Vibrunum erosum* and their neuroprotective and anti-inflammatory activity. Arch. Pharm. Res. 38, 26–34. https://doi.org/10.1007/s12272-014-0358-9.

Isaza, J.H., Ito, H., Yoshida, T., 2001. A flavonol glycoside-lignan ester and accompanying acylated glucosides from *Monochaetum multiflorum*. Phytochemistry 58, 321–327. https://doi.org/10.1016/S0031-9422(01)00247-3.

Jang, H.J., Lee, S., Lee, S.J., Lim, H.J., Jung, K., Kim, Y.H., Lee, S. W., Rho, M.C., 2017. Anti-inflammatory activity of eudesmane-type sesquiterpenoids from *Salvia plebeia*. J. Nat. Prod. 80, 2666–2676. https://doi.org/10.1021/acs.jnatprod.7b00326.

Jeong, E.T., Jin, M.H., Kim, M.S., Chang, Y.H., Park, S.G., 2010. Inhibition of melanogenesis by piceid isolated from *Polygonum cuspidatum*. Arch. Pharm. Res. 33, 1331–1338. https://doi.org/10.1007/s12272-010-0906-x.

Jiao, J., Yang, Y., Wu, Z., Li, B., Zheng, Q., Wei, S., Wang, Y., Yang, M., 2019. Screening cyclooxygenase-2 inhibitors from *Andrographis paniculata* to treat inflammation based on bio-affinity ultrafiltration coupled with UPLC-Q-TOF-MS. Fitoterapia 137,. https://doi.org/10.1016/j.fitote.2019.104259 104259.

Jin, H.Z., Chen, G., Li, X.F., Shen, Y.H., Yan, S.K., Zhang, L., Yang, M., Zhang, W.D., 2009. Flavonoids from *Rhododendron decorum*. Chem. Nat. Compd. 45, 85–86. https://doi.org/10.1007/s10600-009-9245-x.

Kim, S.H., Heo, J.H., Kim, Y.S., Kang, S.S., Choi, J.S., Lee, S.M., 2009. Protective effect of daidzin against d-galactosamine and lipopolysaccharide-induced hepatic failure in mice. Phytother. Res. 23, 701–706. https://doi.org/10.1002/ptr.2710.

Kim, Y.G., Udayanga, K.G., S., Totsuka, N., Weinberg, Jason B., Núñez, G., Shibuya, A.,, 2014. Gut dysbiosis promotes M2 macrophage polarization and allergic airway inflammation via fungi-induced PGE2. Cell Host Microbe 15, 95–102.

Lee, M.H., Son, Y.K., Han, Y.N., 2002a. Tissue factor inhibitory flavonoids from the fruits of *Chaenomeles sinensis*. Arch. Pharm. Res. 25, 842. https://doi.org/10.1007/BF02977002.

Lee, S., Kim, B.K., Cho, S.H., Shin, K.H., 2002b. Phytochemical constituents from the fruits of *Acanthopanax sessiliflorus*. Arch. Pharm. Res. 25, 280. https://doi.org/10.1007/BF02976626.

Lee, M.W., Lee, Y.A., Park, H.M., Toh, S.H., Lee, E.J., Jang, H.D., Kim, Y.H., 2000. Antioxidative phenolic compounds from the roots of *Rhodiola sachalinensis* A. Bor. Arch. Pharm. Res. 23, 455. https://doi.org/10.1007/BF02976571.

Li, M., Bi, J., Lv, B., Zheng, W., Wang, Z., Xiao, W., Sun, Y., Li, E., 2019. An experimental study of the anti-dysmenorrhea effect of Chinese herbal medicines used in Jin Gui Yao Lue. J. Ethnopharmacol. 245, 112–181. https://doi.org/10.1016/j.jep.2019.112181.

Lin, M.H., Liu, H.K., Huang, W.J., Huang, C.C., Wu, T.H., Hsu, F. L., 2011. Evaluation of the potential hypoglycemic and beta-cell protective constituents isolated from *Corni fructus* to tackle insulin-dependent diabetes mellitus. J. Agr. Food Chem. 59, 7743–7751. https://doi.org/10.1021/jf201189r.

Lin, M.Z., Chai, W.M., Zheng, Y.L., Huang, Q., Ouyang, C., 2019. Inhibitory kinetics and mechanism of rifampicin on α-glucosidase: Insights from spectroscopic and molecular docking analyses. Int. J. Biol. Macromol. 122, 1244–1252. https://doi.org/10.1016/j.ijbiomac.2018.09.077.

Liu, Z.B., Sun, C.P., Xu, J.X., Morisseau, C., Hammock, B.D., Qiu, F., 2019. Phytochemical constituents from *Scutellaria baicalensis* in soluble epoxide hydrolase inhibition: Kinetics and interaction mechanism merged with simulations. Int. J. Biol. Macromol. 133, 1187–1193. https://doi.org/10.1016/j.ijbiomac.2019.04.055.

Lu, J.L., Li, W.J., Hou, W.R., Lan, Y., Zhou, H., Yi, L.J., Zeng, Y., Xiang, M., 2012. Study on effect of total coumarins from *Urtica dentata* on dextran sulfate sodium-induced colitis in mice. Chin. J. Chin. Mater. Med. 37, 3316–3320. https://doi.org/10.4268/cjcmm20122133.

Luo, X., Li, L.L., Zhang, S.S., Lu, J.L., Zeng, Y., Zhang, H.Y., Xiang, M., 2011. Therapeutic effects of total coumarins from *Urtica dentata* Hand on collagen-induced arthritis in Balb/c mice. J. Ethnopharmacol. 138, 523–529. https://doi.org/10.1016/j.jep.2011.09.050.

Marwah, R.G., Fatope, M.O., Deadman, M.L., Al-Maqbali, Y.M., Husband, J., 2007. Musanahol: A new aureonitol-related metabolite from a *Chaetomium* sp. Tetrahedron 63, 8174–8180. https://doi.org/10.1016/j.tet.2007.05.119.

Ma, X.M., Liu, Y., Shi, Y.P., 2007. Phenolic derivatives with free-radical-scavenging activities from *Ixeridium gracile* (DC.) Shih. Chem. Biodivers. 4, 2172–2181. https://doi.org/10.1002/cbdv.200790174.

Mohan, M., Hussain, M.A., Khan, F.A., Anindya, R., 2021. Symmetrical and un-symmetrical curcumin analogues as selective COX-1 and COX-2 inhibitor. Eur. J. Pharm. Sci. 160,. https://doi.org/10.1016/j.ejps.2021.105743 150743.

Mujwah, A.A., Mohammed, M.A., Ahmed, M.H., 2010. First isolation of a flavonoid from *Juniperus procera* using ethyl acetate extract. Arab. J. Chem. 3, 85–88. https://doi.org/10.1016/j.arabjc.2010.02.003.

Phongmaykin, J., Kumamoto, T., Ishikawa, T., Suttisri, R., Saifah, E., 2008. A new sesquiterpene and other terpenoid constituents of *Chisocheton penduliflorus*. Arch. Pharm. Res. 31, 21–27. https://doi.org/10.1007/s12272-008-1115-8.

Puig, C., Crespo, M.I., Godessart, N., Feixas, J., Ibarzo, J., Jiménez, J. M., Soca, L., Cardelús, I., Heredia, A., Miralpeix, M., Puig, J., Beleta, J., Huerta, J.M., López, M., Segarra, V., Ryder, H., Palacios, J.M., 2000. Synthesis and biological evaluation of 3,4-diaryloxazolones: a new class of orally active cyclooxygenase-2 inhibitors. J. Med. Chem. 43, 214–223. https://doi.org/10.1021/jm991106b.

Qin, F.Y., Zhang, H.X., Di, Q.Q., Wang, Y., Yan, Y.M., Chen, W.L., Cheng, Y.X., 2020. *Ganoderma cochlear* metabolites as probes to identify a COX-2 active site and as *in vitro* and *in vivo* anti-inflammatory agents. Org. Lett. 22, 2574–2578. https://doi.org/10.1021/acs.orglett.0c00452.

Rasouli, H., Ghazvini, S.M.B.H., Yarani, R., Altintas, A., Jooneghani, S.G.N., Ramalho, T.C., 2020. Deciphering inhibitory activity of flavonoids against tau protein kinases: a coupled molecular docking and quantum chemical study. J. Biomol. Struct. Dyn. https://doi.org/10.1080/07391102.2020.1814868.

Righi, G., Silvestri, I.P., Barontini, M., Crisante, F., Di Manno, A., Pelagalli, R., Bovicelli, P., 2012. Efficient synthesis of scutellarein. Nat. Prod. Res. 26, 1278–1284. https://doi.org/10.1080/14786419.2011.566224.

Rostamian, M., Farasat, A., Lorestani, K.C., Zargaran, F.N., Ghadiri, K., Akya, A., 2020. Immunoinformatics and molecular dynamics studies to predict T-cell-specific epitopes of four *Klebsiella pneumoniae* fimbriae antigens. J. Biomol. Struct. Dyn. 14, 1–11. https://doi.org/10.1080/07391102.2020.1810126.

Seidel, V., Bailleul, F., Waterman, P.G., 2000. (Rel)-1β,2α-di-(2,4-dihydroxy-6-methoxybenzoyl)-3*β*, 4α-di-(4-methoxyphenyl)-cyclobutane and other flavonoids from the aerial parts of *Goniothalamus gardneri* and *Goniothalamus thwaitesii*. Phytochemistry 55, 439–446. https://doi.org/10.1016/S0031-9422(00)00346-0.

Song, L.R., 2005. Chinese herbal medicine (Miao Yao Juan). Guizhou Science and Technology Publishing House.

Souza, J.N.S., Silva, E.M., da Silva, M.N., Arruda, M.S.P., Larondellea, Y., Rogez, H., 2007. Identification and antioxidant activity of several flavonoids of *Inga edulis* leaves. J. Braz. Chem. Soc. 18, 1276–1280. https://doi.org/10.1590/S0103-50532007000600025.

State Drug Administration, 2002a. Compendium of national standards for Chinese patent medicines division of orthopedics and traumatology. State Drug Administration, Beijing.

State Drug Administration, 2002b. Compilation of national standards for proprietary Chinese medicine. State Drug Administration, Beijing.

Su, X.C., Chen, L., Aisa, H.A., 2008. Flavonoids and sterols from *Alhagi sparsifolia* 365–365 Chem. Nat. Compd. 44. https://doi.org/10.1007/s10600-008-9064-5.

Su, Z.Q., Zhao, Z.Y., Xie, S.N., Hou, W.R., Tao, E., Xiang, M., 2009. Effects of analgesia, anti-inflammation and immunosuppression of acetic ether extract of Chinese medicine Honghuoma. Chin. Pharmacol. Bull. 25, 559–560. https://doi.org/10.3321/j.issn:1001-1978.2009.04.037.

Sun, C.P., Tian, X.G., Feng, L., Wang, C., Li, J.X., Huo, X.K., Zhao, W.Y., Ning, J., Yu, Z.L., Deng, S., Zhang, B.J., Lv, X., Hou, J., Ma, X.C., 2021. Inhibition of gut bacterial β-glucuronidase by chemical components from black tea: Inhibition interactions and molecular mechanism. Arab. J. Chem. 14,. https://doi.org/10.1016/j.arabjc.2021.103457 103457.

Thomas, M.J., Pryor, W.A., 1980. Singlet oxygen oxidation of methyl linoleate: Isolation and characterization of the NaBH4-reduced products. Lipids 15, 544–548. https://doi.org/10.1007/BF02534228.

Tian, J., Zhao, Y.M., Luan, X.H., 2005. Studies on the chemical constitutents in herb of *Verbena officinalis*. Chin. J. Chin. Mater. Med. 30, 268–269.

Wang, H., Nair, M.G., Strasburg, G.M., Booren, A.M., Gray, J.I., 1999. Novel antioxidant compounds from Tart cherries (*Prunus cerasus*). J. Nat. Prod. 62, 86–88. https://doi.org/10.1021/np980268s.

Wang, J.L., Limburg, D., Graneto, M.J., Springer, J., Hamper, J.R., Liao, S., Pawlitz, J.L., Kurumbail, R.G., Maziasz, T., Talley, J.J., Kiefer, J.R., Carter, J., 2010. The novel benzopyran class of selective cyclooxygenase-2 inhibitors. Part 2: the second clinical candidate having a shorter and favorable human half-life. Bioorg. Med. Chem. Lett. 20, 7159–7163 https://doi.10.1016/j.bmcl.2010.07.054.

Wang, J., Lu, J., Lan, Y., Zhou, H., Li, W., Xiang, M., 2013. Total coumarins from *Urtica dentata* Hand prevent murine autoimmune diabetes via suppression of the TLR4-signaling pathways. J. Ethnopharmacol. 146, 379–392. https://doi.org/10.1016/j.jep.2013.01.009.

Wang, R.R., Gu, Q., Wang, Y.H., Zhang, X.M., Yang, L.M., Zhou, J., Chen, J.J., Zheng, Y.T., 2008. Anti-HIV-1 activities of compounds isolated from the medicinal plant *Rhus chinensis*. J. Ethnopharmacol. 117, 249–256. https://doi.org/10.1016/j.jep.2008.01.037.

Wang, Y.L., Dong, P.P., Liang, J.H., Li, N., Sun, C.P., Tian, X.G., Huo, X.K., Zhang, B.J., Ma, X.C., Lv, C.Z., 2018. Phytochemical constituents from *Uncaria rhynchophylla* in human carboxylesterase 2 inhibition: Kinetics and interaction mechanism merged with docking simulations. Phytomedicine 51, 120–127. https://doi.org/10.1016/j.phymed.2018.10.006.

Wei, X.H., Yang, S.J., Liang, N., Hu, D.Y., Jin, L.H., Xue, W., Yang, S., 2013. Chemical constituents of *Caesalpinia decapetala* (Roth) Alston. Molecules 18, 1325–1336. https://doi.org/10.3390/molecules18011325.

Xian, D.L., Huang, K.L., Hu, W.G., Xiao, J.Y., Jiao, F.P., 2007. Evaluation of ferulic acid-biomembrane interaction by liposome electrokinetic chromatography. Chin. J. Anal. Chem. 35, 1521–1524. https://doi.org/10.1016/S1872-2040(07)60090-5.

Xiang, M., Hou, W.R., Xie, S.N., Zhang, W.D., Wang, X., 2009. Immunosuppressive effects of an ethyl acetate extract from *Urtica dentata* Hand on skin allograft rejection. J. Ethnopharmacol. 126, 57–63. https://doi.org/10.1016/j.jep.2009.08.011.

Xu, Y.C., Wang, Y., Wu, D., He, W.W., Wang, L.P., Zhu, W.M., 2021. P-terphenyls from *Aspergillus* sp. GZWMJZ-055: Identification, derivation, antioxidant and α-glycosidase inhibitory activities.

Front. Microbiol. 12,. https://doi.org/10.3389/fmicb.2021.654963 654963.

Yang, M.C., Choi, S.Z., Lee, S.O., Chung, A.K., Nam, J.H., Lee, K.H., Lee, K.R., 2003. Flavonoid constituents and their antioxidant activity of *Laportea bulbifera* Weddell. Kor. J. Pharmacogn. 34, 18–24.

Yang, H.J., Li, G., 2019. Report on the Scientific and Technological Competitiveness of Large Varieties of Traditional Chinese Medicine. The People's Medical Publishing House.

Yu, B.C., Yang, M.C., Lee, K.H., Kim, K.H., Lee, K.R., 2007. Norsesquiterpene and steroid constituents of *Humulus japonicus*. Nat. Prod. Science 13, 332–336.

Yuan, T., Li, L., Zhang, Y., Seeram, N.P., 2013. Pasteurized and sterilized maple sap as functional beverages: Chemical composition and antioxidant activities. J. Funct. Foods 5, 1582–1590. https://doi.org/10.1016/j.jff.2013.06.009.

Yue, Z., Qin, H., Li, Y., Sun, Y., Wang, Z., Yang, T., Liu, L., Wang, M., Feng, F., Mei, Q., 2013. Chemical constituents of the root of *Jasminum giraldii*. Molecules 18, 4766–4775. https://doi.org/10.3390/molecules18044766.

Zhang, H., Xu, H.H., Song, Z.J., Chen, L.Y., Wen, H.J., 2012. Molluscicidal activity of *Aglaia duperreana* and the constituents of its twigs and leaves. Fitoterapia 83, 1081–1086. https://doi.org/10.1016/j.fitote.2012.05.003.

Zhang, N., Chu, X.Q., Jiang, J.Q., 2015. Chemical constituents in ethyl acetate extract from *Physalis alkekengi* var. *franchetii*. Chin. Tradit. Herbal. Drugs. 46, 1120–1124. https://doi.org/10.7501/j.issn.0253-2670.2015.08.004.

Zhang, Y., Lu, X., Li, B., Yu, D.Y., Feng, B.M., 2018. Flavonoids from Laportea bulbifera and their anti-N1 neuraminidase activities. J. Shenyang Pharm. Univ. 35, 931–935. +942.

Zhao, H.T., Dong, J., Lafleur, K., Nevado, C., Caflisch, A., 2012. Discovery of a novel chemotype of tyrosine kinase inhibitors by fragment-based docking and molecular dynamics. ACS Med. Chem. Lett. 2012 (3), 834–838 https://10.1021/ml3001984.

Zhao, W.Y., Zhang, X.Y., Zhou, M.R., Tian, X.G., Lv, X., Zhang, H. L., Deng, S., Zhang, B.J., Sun, C.P., Ma, X.C., 2021. Natural soluble epoxide hydrolase inhibitors from *Alisma orientale* and their potential mechanism with soluble epoxide hydrolase. Int. J. Biol. Macromol. 183, 811–817. https://doi.org/10.1016/j.ijbiomac.2021.04.187.

Zhu, Z., Ma, L., Zhu, H.Y., Yang, X.S., Hao, X.J., 2011. Studies on the chemical constituents of *Laportea bulbifera*. Chin. Med. Mat. 34, 223–225. https://doi.org/10.1007/s10008-010-1224-4.

Zou, X., Liang, J., Ding, L.S., Peng, S.L., 2006. Studies on chemical constituents of *Paederia scandense*. Chin. J. Chin. Mater. Med. 31, 1436–1441.